Electronic Supplementary Material (ESI) for Nanoscale.
This journal is © The Royal Society of Chemistry 2015

Supporting Information for :

Direct synthesis of graphene 3D-coated Cu nanosilks network for antioxidant transparent conducting electrode

Hongmei Xu[1], Huachun Wang[1], Chenping Wu[1], Na Lin[1,5], Abdul Majid Soomro[1], Huizhang Guo[3], Chuan Liu[4], Xiaodong Yang[4], Yaping Wu[1,a)], Duanjun Cai[1,2,a)], and JunYong Kang[1]

[1] *Fujian Key Laboratory of Semiconductor Materials and Applications, School of Physics and Mechanical & Electrical Engineering, Xiamen University, Xiamen 361005, China.*

[2] *Institute of Photonics and Optoelectronics and Department of Electrical Engineering, National Taiwan University, 1, Roosevelt Road, Section 4, Taipei 10617, Taiwan.*

[3] *Institute for Building Materials, ETH Zurich, Zurich, Switzerland.*

[4] *State Key Laboratory of Physical Chemistry of Solid Surfaces, College of Chemistry and Chemical Engineering, Xiamen University, Xiamen 361005,China.*

[5] *Xiamen Industrial & Commercial School, Jimei district, Xiamen 361024, China.*

a) E-mail: dcai@xmu.edu.cn , ypwu@xmu.edu.cn

Mechanism discussions

The synthesis process and mechanism showed that the Ni(0) atoms in the solution play the role of catalyst for reducing the Cu^{2+} ions into Cu atoms and then, the Cu nanocrystal seeds nucleate and grow along [1-10] direction into Cu NSs. Most importantly, because of the use of $CuCl_2$ as reaction precursor, elongation of the super-fine Cu NS was carried out with the presence of Cl^- ions by passivating the radial growth. As shown in **Fig. S1**, the Auger electron spectroscopy (AES) measurement demonstrates the existence of the Cl on the as-grown Cu NSs networks. This suggests that the Cl^- ions will attach onto the {100} and {111} sidewall facets and lead to a strongly anisotropic growth by limiting the radial growth rate. During the synthesis of Cu NSs, the Cl^- ion plays the critical role in minimizing the diameter of NS.

By using percolation technique, the Cu NS networks can be imprinted onto any target substrates such as quartz glass, Polyethylene terephthalate (PET), or semiconductor wafers in absence of any surface modification or bonding epoxy. **Fig. S2** shows the processes of suction filtration and imprint. With this technique, the transparent conductive film in unlimited size and various shape can be easily achieved and furthermore, desired pattern structure could also be made through photolithography method. **Fig. S3** shows the imprinted Cu NS film on 2” sapphire substrate, which already meets the requirement of the size of industrial mass production of optoelectronic devices. The transferred conductive film has a good uniformity, excellent dispersion and tight interlacing, as shown in **Fig. S4**. The graphene coated Cu NSs network is in the same large size as that achieved with pure Cu NSs film.

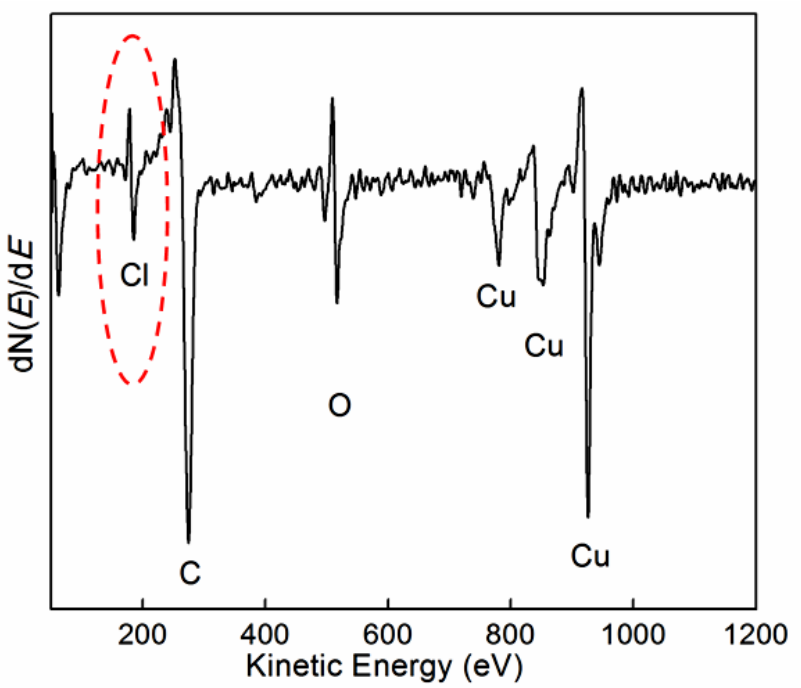

Fig. S1. Differential AES spectrum of Cu NSs. The the presence of Cl demonstrates the Cl^- surfactants adsorbed on the Cu NS sidewall. The signal of oxygen may result from the surface-absorbed CO_2, H_2O and O_2.

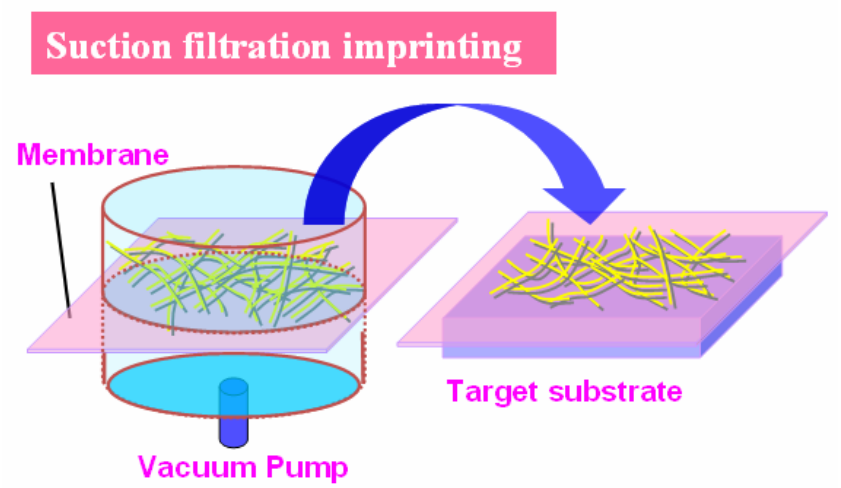

Fig. S2. Schematic illustrating the suction filtration and imprint processes of Cu NS conductive film.

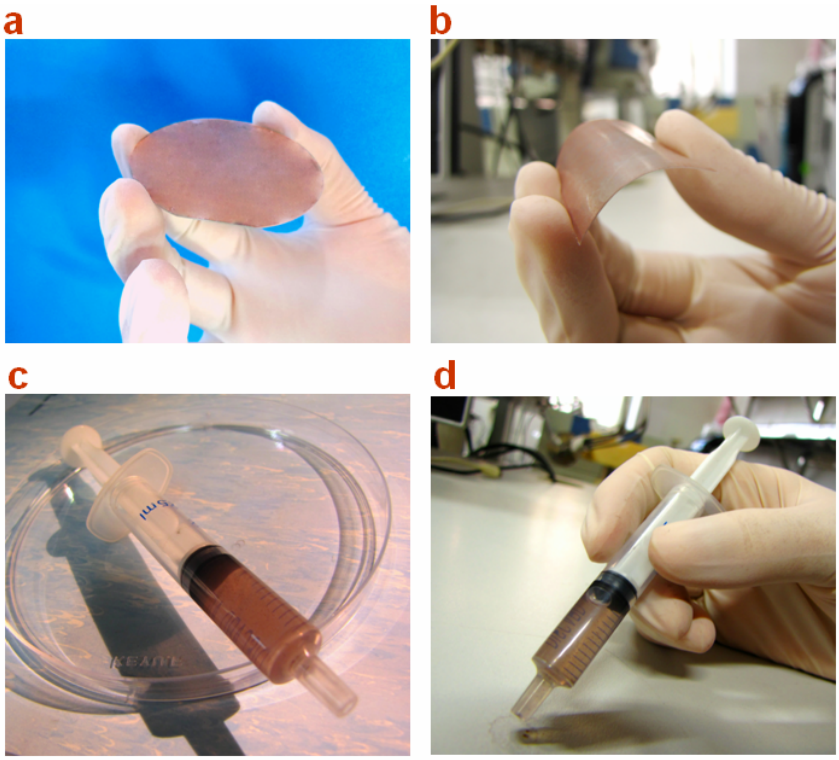

Fig. S3. Photographs of unlimited-size TEs imprinted with Cu NSs ink. (a) Imprinted transparent conducting film on 2” sapphire substrate, (b) flexible transparent film on PET, and (c) and (d) Cu NSs ink as conductive adhesive epoxy filled in injector, which could be written on any substrate.

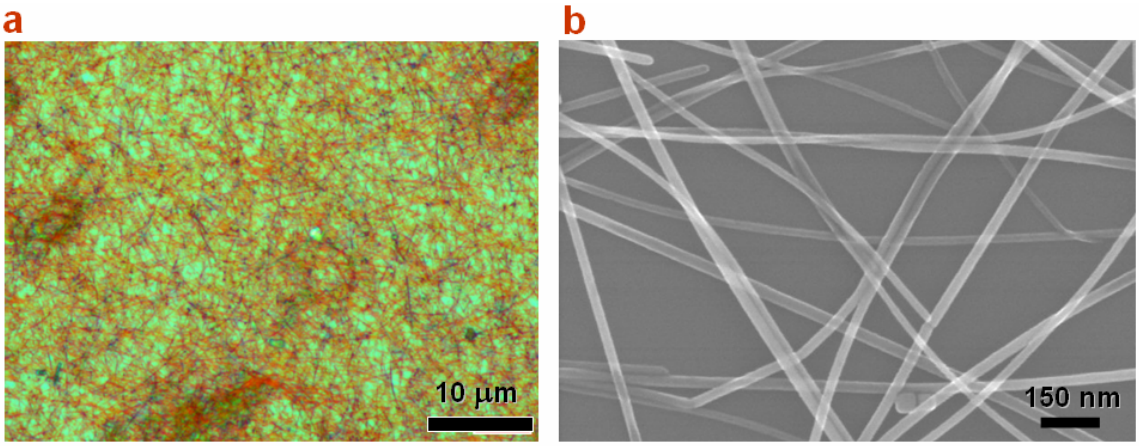

Fig. S4. Optical (a) and SEM (b) of transferred Cu NS network on Si substrate. The uniformity and interlacing Cu NSs as complete network is shown.

A series of Cu NS network TEs in various thicknesses were prepared by using Cu NS inks in different concentration and their transmittances were measured, as shown in **Fig. S5**. One can see that the transmittance is increasing with decreasing the concentration of the Cu NS ink. Most importantly, the transmittance keeps nearly constant over the broad wavelength range from 200 nm to 3000 nm, which covers the deep ultraviolet to the near infrared region. Such a wide window for light transmission demonstrates the potential of application of Cu NS TEs in both UV lighting, visible lighting and even photovoltaic systems.

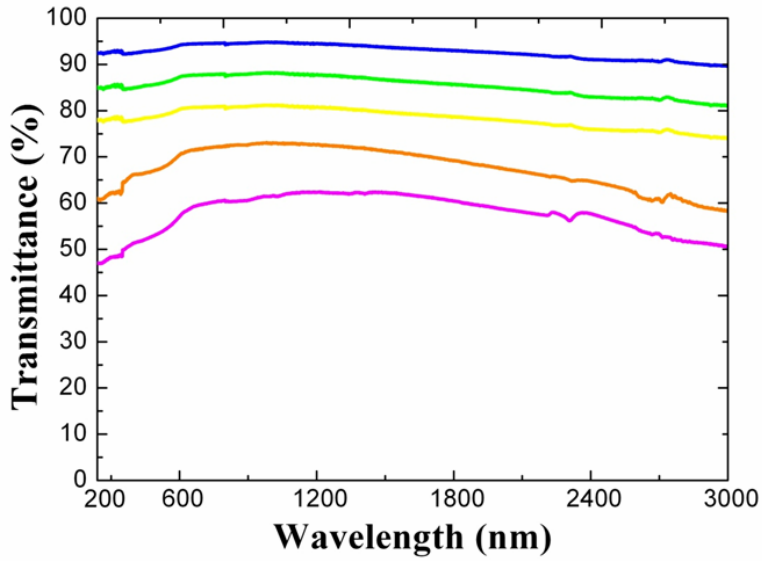

Fig. S5. UV-Vis-NIR transmission spectra for the Cu NS TEs fabricated with Cu NS inks in various concentrations. A broad transparency from 200 to 3000 nm is achieved.

Direct 3D-coating of graphene on Cu NSs network

The Cu NSs were systematically annealed under vacuum at increasing temperatures from 200 ºC to 1000 ºC. **Fig. S6** shows the SEM images of these annealed samples. One can see that at 200 ºC and 400 ºC the structure of Cu NSs remains stable whereas they get melted and aggregated into clusters when the annealing temperature goes beyond 700 ºC. When the annealing temperature reaches 900 ºC and above, the clustering of Cu NSs becomes extremely serious. In principles, the saturation vapor pressure of Cu is increasing with the increase of the environment temperature, as listed in **Table I**.

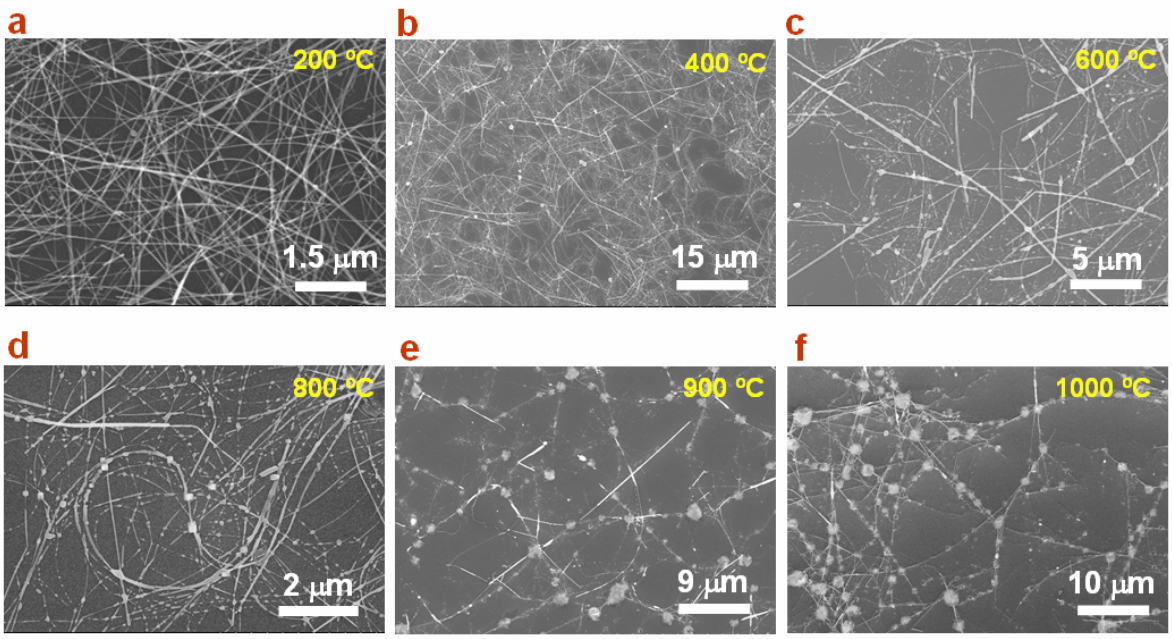

Fig. S6. SEM images of Cu NSs after annealing at different temperatures for 5 min. It shows that the Cu NSs start to melt over 600 ºC. The melting point was determined to be at around 700 ºC.

Table 1 Temperature for Vapor Pressure of copper.

Pressure (Torr)	**10^{-8}**	**10^{-7}**	**10^{-6}**	**10^{-5}**	**10^{-4}**	**10^{-3}**	**10^{-2}**	**10^{-1}**	**1**
Temperature (°C)	722	787	852	937	1027	1132	1257	1417	1617

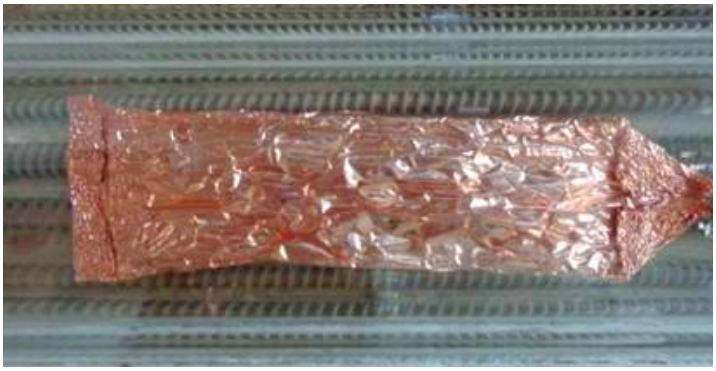

Fig. S7. Picture of Cu capsule used for producing higher vapor pressure of Cu to protect the Cu NSs from melting.

In order to increase the vapor pressure of Cu on Cu NSs, the method of "Cu capsule" is proposed to produce higher saturation vapor pressure, which may prevent the melting of Cu NSs at high temperature and under vacuum. **Fig. S7** illustrates the photo of one type of Cu capsules which contains the Cu NSs film and is put in the quartz tube. The openings of the capsule should be tightly folded or even sealed so that the vapor pressure inside the capsule could be effectively increased under vacuum. As a result, the TEM image confirms the tight and uniform 3D-coating of graphene on the Cu NS surfaces. The coating layer well follows the surface morphology of NSs due to the catalysis of Cu for graphene formation.

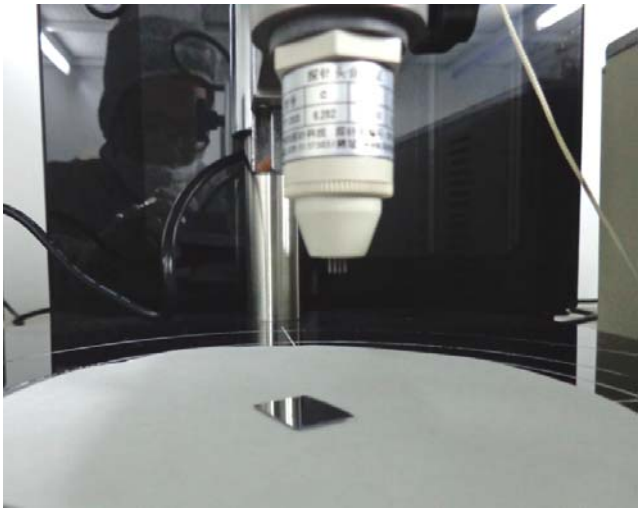

Fig. S8. Photograph of the system of 4-wire resistivity measurement.

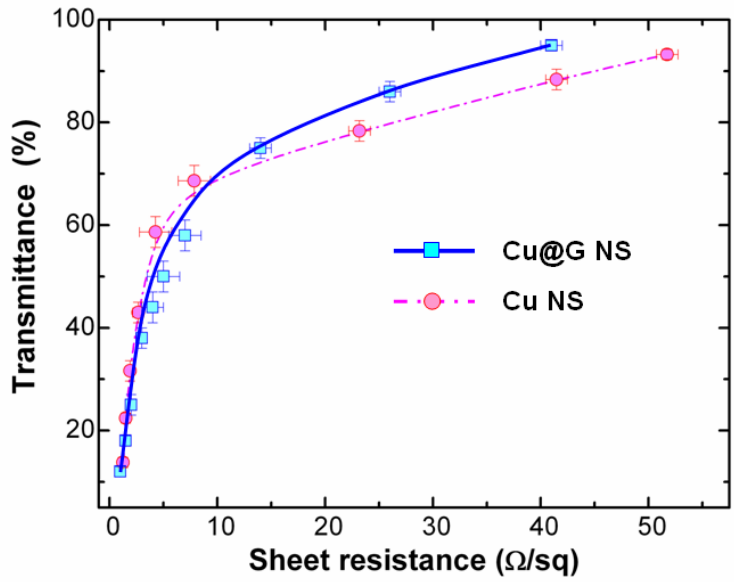

Fig. S9. Transmittance as a function of sheet resistance for samples of Cu NS and Cu@G NS.

We also found that in the range of 3 ~ 10 ohm/sq, as shown in Fig. S9, the transmittance of the Cu@G NS is lower than that of the Cu NS network. We can see that this region actually appears to be the critical turning point of T-R curve for both samples. Over this turning point the T-R relation changes drastically. This means that at this turning point the T-R relation become a little bit unstable, which could possess both features on both sides of the turning points. Hence, we found that in this region the samples with slightly different transmittance may have the same resistance, which is a deviation.

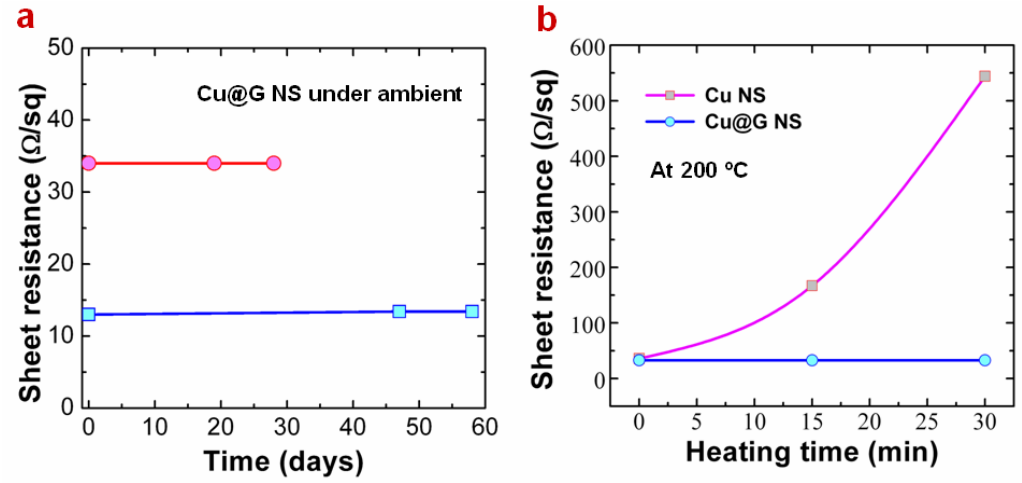

Fig. S10. Sheet resistance as a function of time. (a) Sheet resistance of Cu@G NS network put under ambient over two month, and (b) variation of sheet resistance under 200 °C in air.

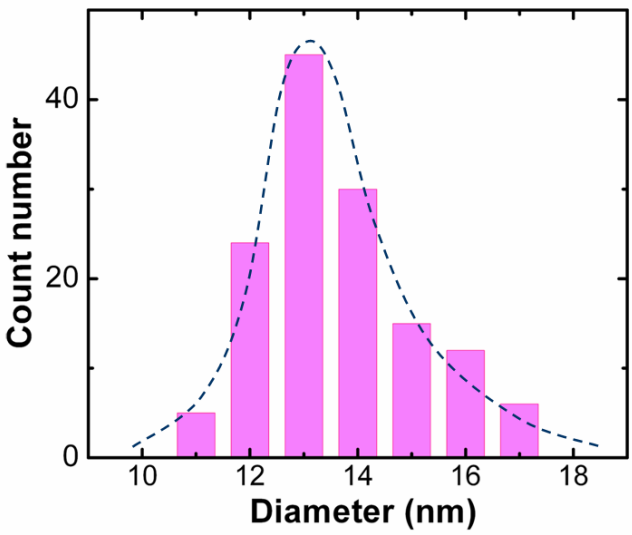

Fig. S11. Diameter distribution of Cu NS.

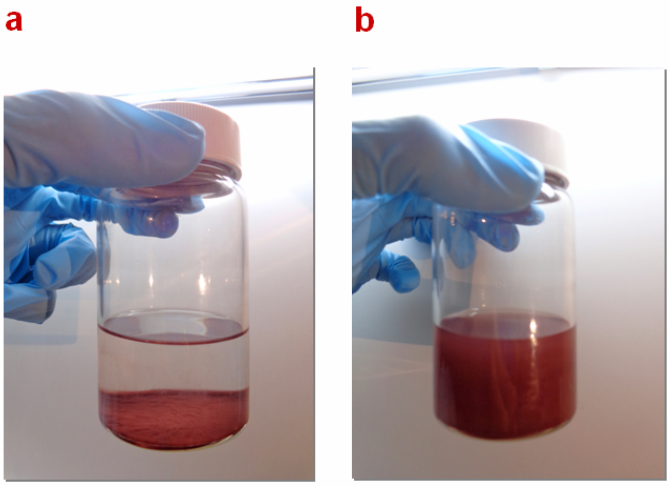

Fig. S12. Photographs of Cu NS kept in hexane solution for two months (a) and after dispersion by bath sonication (b).

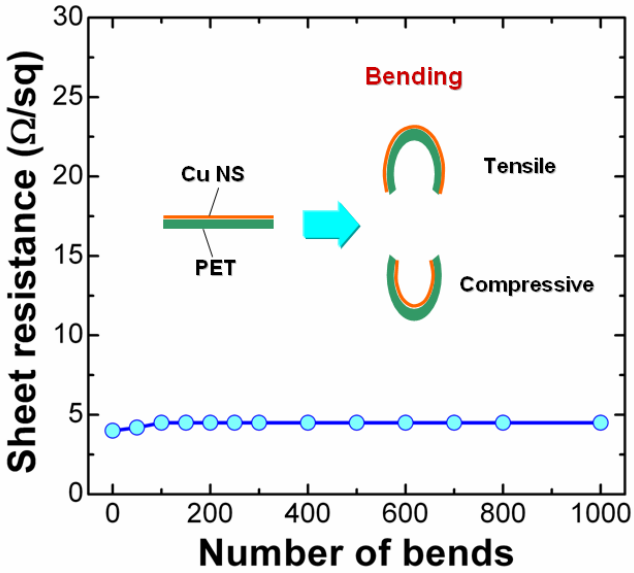

Fig. S13. Sheet resistance of Cu NS network as a function of number of bends by 180°.

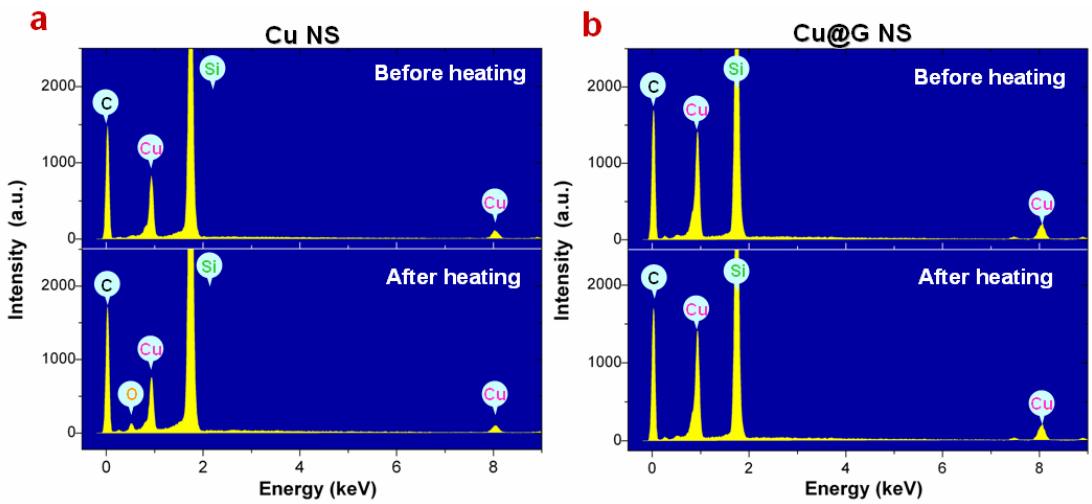

Fig. S14. EDS of Cu NS (a) and Cu@G NS (b) before and after heating at 200 °C in air.

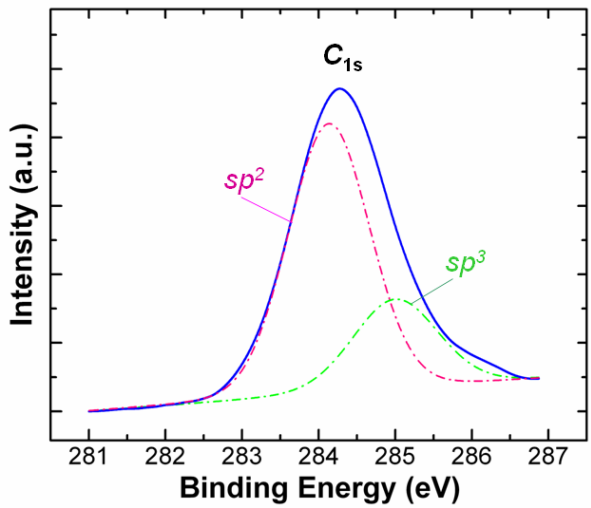

Fig. S15. XPS spectrum of Cu@G NS, showing the sp2/sp3 hybridization ratio of C-C bonding.

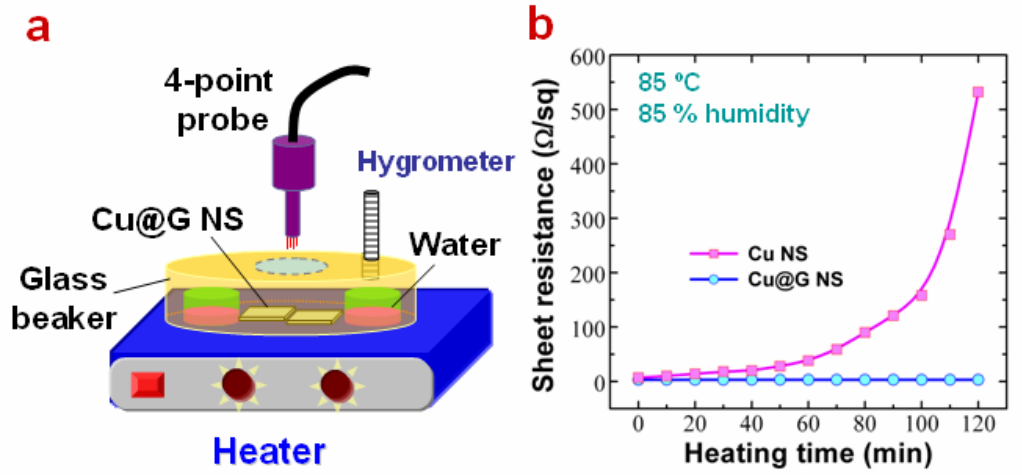

Fig. S16. (a) Schematic of the setup of stability measurements under high temperature and high humidity, and (b) sheet resistance as a function of heating time.

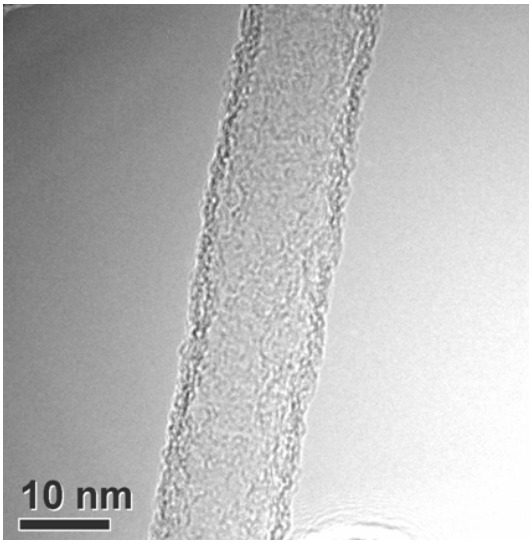

Fig. S17. TEM image of graphene shell tube by removing Cu NS.

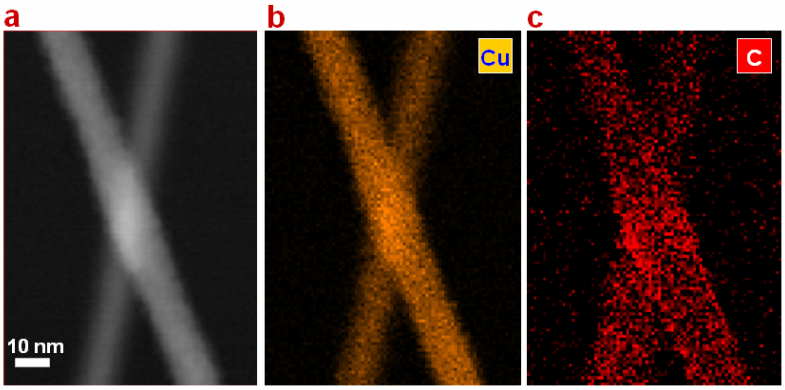

Fig. S18. (a) STEM image interlaced Cu@G NSs, and (b) and (c) the elemental mapping of Cu and C, respectively.

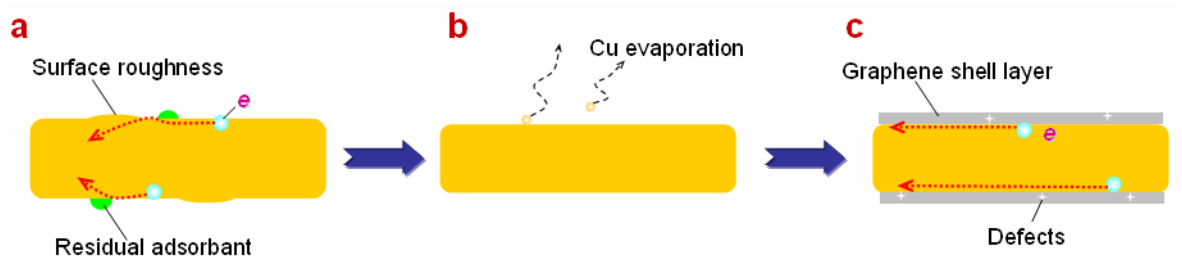

Fig. S19. Schematics of the electron transportation along Cu@G NSs. (a) Electron transport and scattering on Cu NS surface. Existence of residual adsorbants and slight surface roughness after low-temperature annealing will give rise to the electron scattering and limit the conductivity of Cu NS TE. (b) Cu evaporation at higher temperature (700 ^{o}C) further smoothens the surface of Cu NS and reduces diameter. (c) Fast electron transport along the graphene/Cu NS interface. Defects and grain boundaries in graphene shell layer do not significantly affect the electron movement on the Cu NS surface.